Lower hybrid drift instability in a neutral sheet with O^+ ions

Feng Huang, Yinhua Chen, Hai-Ou Peng, Ju-Gao Zheng, Gui-Fen Shi, and Zu-Quan Hu
Key Laboratory of Basic Physics, Chinese Academy of Science, and Department of Modern Physics, University of Science and Technology of China, 230026 Hefei, People's Republic of China

M. Y. Yu
Institute for Fusion Theory and Simulation, Department of Physics, Zhejiang University, 310027 Hangzhou, China and Institute of Theoretical Physics I, Ruhr University, D-44780 Bochum, Germany

(Received 25 June 2009; revised manuscript received 13 September 2009; published 3 November 2009)

The electromagnetic lower-hybrid drift instability (LHDI) in the intermediate-wavelength regime $k_y\sqrt{\rho_i\rho_e} \sim 1$, where k_y and $\rho_{e,i}$ are the wave vector and the electron and ion gyroradii, respectively, in a thin plasma sheet containing electrons and H^+ and O^+ ions is examined using kinetic theory. It is shown that the growth rate of the LHDI first decreases and then increases with increase in the O^+ content and temperature, with a minimum at a moderate level of the latter. The results can be relevant to understanding magnetic reconnection in the presence of LHDI.

DOI: 10.1103/PhysRevE.80.056401 PACS number(s): 52.35.Qz, 52.35.Hr

I. INTRODUCTION

It is well-known that the presence of impurity species in plasma can lead to new phenomena as well as modify known ones, such as new waves and instabilities, minority-ion heating, heavy-ion acceleration, modified magnetic reconnection, etc. [1–16]. Observations showed that O^+ ions are often present in plasma sheets [6,7,10–13], so that magnetic reconnection in plasmas containing O^+ ions has attracted considerable attention [4,5,14]. The lower-hybrid drift instability (LHDI) has often been invoked as a source for anomalous resistivity in magnetic reconnection and related phenomena [15–27]. The electrostatic LHDI was first considered by Krall and Liewer [20], and the resulting anomalous resistivity by Gladd and Davidson [23]. Daughton [18] found that the mode structure of the LHDI can have a significant electromagnetic component localized in the center region of the sheet, where electromagnetic fluctuations can potentially affect magnetic reconnection. Recently, Wang *et al.* [27] considered obliquely propagating LHD waves and found that the perpendicular propagating modes are responsible for enhancing the anomalous resistivity.

In this paper, we consider the effect of O^+ ions on the linear LHDI in a current sheet using a Vlasov-Maxwell kinetic model including magnetic field perturbations. The orbit integrals are treated numerically and the corresponding eigenvalue problem consisting of coupled integrodifferential equations is solved by using a finite-element representation of the eigenfunction [18,28–30]. It is found that the dependence of the growth rate of the fastest growing mode on the O^+ content and temperature is not monotonic.

In Sec. II, the self-consistent Vlasov steady-state of a three-species neutral sheet is obtained, and in Sec. III the dispersion relation of the LHDI considered. In Sec. IV, the corresponding numerical results are presented. The results are discussed in Sec. V.

II. STEADY-STATE HARRIS SHEET WITH THREE SPECIES OF PARTICLES

We consider a Harris equilibrium [16], where the magnetic field given by $\vec{B}_z(x)=B_0\tanh(x/L)\vec{e}_z$, where L is the half thickness of the sheet, and there is no electric field ($\vec{E}_0=0$). The plasma is assumed to be in local thermodynamic equilibrium [16], with the particle distribution functions satisfying the local Maxwellian

$$f_{0s}=\frac{n_s}{\pi^{3/2}v_{ts}^3}\exp\left[-\frac{v_x^2+(v_y-U_s)^2+v_z^2}{v_{ts}^2}\right], \tag{1}$$

where $n_s(x)=\int d\vec{v}f_{0s}=n_{0s}\,\mathrm{sech}^2(x/L)$ is the density, $U_s=\langle v_{ys}\rangle=\frac{1}{n_s}\int_{-\infty}^{\infty}v_y f_{0s}(x,\vec{v})d\vec{v}$ is the transverse fluid velocity, $v_{ts}=\sqrt{T_s/m_s}$ is the thermal speed, and $T_s=\frac{m_s}{3}\langle|\vec{v}-U\vec{e}_y|^2\rangle=\frac{m_s}{3n_s}\int_{-\infty}^{\infty}|\vec{v}-U\vec{e}_y|^2 f_{0s}(x,\vec{v})d\vec{v}$ is the temperature of the species $s=i,e,O^+$ (protons, electrons, and O^+ ions). The integrals in U_s, T_s, and n_s lead to x-dependent expressions of the same forms, so that U_s and T_s (thus also v_{ts}) are constants [16]. Because of the charge neutrality condition $\Sigma_s q_s n_s=0$, where q_s is the charge, one has $en_{0i}-en_{0e}+q_{O^+}n_{0O^+}=0$, and $-U_i/T_i=-U_e/T_e=q_{O^+}U_{O^+}/eT_{O^+}$ [30]. Steady-state pressure balance also leads to $B_0^2=8\pi(T_i n_{0i}+T_e n_{0e}+T_{O^+}n_{0O^+})$ [16]. The Harris current sheet in a three-species plasma here is an exact solution to the steady-state Vlasov-Maxwell equations.

III. DISPERSION RELATION

We now investigate nonlocal linear LHDI in the Harris current sheet using a finite-element representation of the eigenfunction in the corresponding eigenvalue problem consisting of a set of integrodifferential equations [18,28]. The linearized Vlasov equation is

$$\frac{\partial f_{1s}}{\partial t}+\vec{v}\cdot\nabla f_{1s}+\frac{\vec{v}\times\vec{B}_0}{c}\cdot\nabla_v f_{1s} = -\frac{q_s}{m_s}\left(\vec{E}_1+\frac{\vec{v}\times\vec{B}_1}{c}\right)\cdot\nabla_v f_{0s}, \tag{2}$$

where f_{0s} is given by Eq. (1) and f_{1s} is the perturbed distribution function and $\vec{E}_1$ and $\vec{B}_1$ are the perturbed electric and magnetic fields. We can write $\vec{E}_1$ and $\vec{B}_1$ in terms of the scalar and vector potentials as

$$\vec{E}_1 = -\nabla\phi_1 - \frac{1}{c}\frac{\partial \vec{A}_1}{\partial t} \quad \text{and} \quad \vec{B}_1 = \nabla \times \vec{A}_1. \tag{3}$$

The perturbation quantities are assumed to have a Fourier representation in the y direction

$$Q_1 = \tilde{Q}(x)\exp(-i\omega t + ik_y y), \tag{4}$$

where ω and k_y correspond to the wave frequency and wave vector, respectively. Integrating along the unperturbed particle orbits, we obtain the perturbed distribution function

$$f_{1s} = -\frac{q_s f_{0s}}{T_s}\left[\tilde{\phi}(x) - \frac{U_s}{c}\tilde{A}_y(x) - i(\omega - k_y U_s)S\right], \tag{5}$$

where $S = \int_{-\infty}^{0}[\frac{1}{c}\tilde{\vec{A}}(x')\cdot\vec{v}' - \tilde{\phi}(x')]\exp[-i\omega\tau + ik_y(y'-y)]d\tau$, and $x'(\tau)$, $y'(\tau)$, and $\vec{v}'(\tau)$ are determined by the particle trajectories in the Harris sheet. The initial (at $\tau=0$) conditions are $x'=x$, $y'=y$, and $\vec{v}'=\vec{v}$. From Eq. (5), one can obtain the perturbed charge and current densities

$$\tilde{\rho} = \sum_s \left[\frac{q_s^2 n_s}{T_s}\left(\tilde{\phi} - \frac{U_s}{c}\tilde{A}_y\right) - i\frac{q_s^2(\omega - k_y u_s)}{T_s}\int f_{0s} S d\vec{v}\right], \tag{6}$$

$$\tilde{\vec{J}} = \sum_s \left[\frac{q_s^2 n_s U_s}{T_s}\left(\tilde{\phi} - \frac{U_s}{c}\tilde{A}_y\right) - i\frac{q_s^2(\omega - k_y u_s)}{T_s}\int f_{0s}\vec{v} S d\vec{v}\right], \tag{7}$$

respectively.

A charged particle in the Harris sheet has three constants of motion, namely, the z-direction momentum $p_{zs}=m_s v_z$, the total y-direction momentum $p_{ys}=m_s v_y + q_s A_y/c$, and the total energy $H_s=\frac{1}{2}m_s(v_x^2+v_y^2+v_z^2)$, where $A_y=\int B_z(x)dx$ is the vector potential and c is the speed of light in vacuum. Thus, the x component of the equation of motion can be written as

$$m_s\frac{dv_x}{dt} = -\frac{1}{2m_s}\frac{\partial}{\partial x}\left(p_{ys} - \frac{q_s A_{ys}(x)}{c}\right)^2, \tag{8}$$

from which we can see that the particle can be trapped in the x direction by a potential well and bounce with the speed $v_x=\sqrt{v_\perp^2 - (\frac{p_{ys}}{m_s} - \frac{q_s A_y(x)}{cm_s})^2}$ between two turning points where $v_x=0$. That is, the particle orbit is periodic in x', v_x', and v_y' $(=p_{ys}/m_s - q_s A_y(x')/m_s c)$, with the period t_p determined by the initial conditions [18,28]. In the z direction, we have the free-flight trajectory given by $v_z'=v_z$ and $z'=z+v_z\tau$. The period of the particle orbit is given by $t_p=2\int_{x_1}^{x_2}v_x^{-1}(x)dx$, where x_1 and x_2 are the two turning points where $v_x=0$. The y component $y'(\tau)$ of the trajectory is not periodic. However, it has the property $y'(\tau+nt_p)=n\Delta y + y'(\tau)$, where n is an positive integer and $\Delta y=\int_{-t_p}^{0}v_y'(\tau)d\tau$ is a net drift during one period of the motion. Using this relation and the x-direction periodicity, one obtains

$$\tilde{S} \equiv \frac{1}{1-\exp(i\omega t_p + ik_y\Delta y)}\int_{-t_p}^{0}\left(\frac{1}{c}\tilde{A}(x')\cdot\vec{v}' - \tilde{\phi}(x')\right) \times \exp[-i\omega\tau + i\vec{k}\cdot(y'-y)]d\tau, \tag{9}$$

which can be readily integrated. The equations are completed by the Maxwell's equations

$$\nabla^2\phi_1 - \frac{1}{c^2}\frac{\partial^2\phi_1}{\partial t^2} = -4\pi\rho_1,$$

$$\nabla^2\vec{A}_1 - \frac{1}{c^2}\frac{\partial^2\vec{A}}{\partial t^2} = -4\pi\vec{J}_1, \tag{10}$$

where ρ_1 and $\vec{J}_1$ are given by Eqs. (6) and (7), respectively, and the Lorentz gauge has been used.

The integrodifferential Eq. (10) can be solved numerically by first constructing a basis set of functions that satisfy the boundary conditions [18,28]. Accordingly, the perturbation potentials $\tilde{\phi}(x)$ and $\tilde{\vec{A}}(x)$ are expanded in terms of a series of basis functions as follows:

$$\tilde{\phi}(x) = \sum_{n=1}^{N} C_n\psi_n(x), \quad \tilde{A}_x(x) = \sum_{n=1}^{N} C_{N+n}\psi_n(x),$$

$$\tilde{A}_y(x) = \sum_{n=1}^{N} C_{2N+n}\psi_n(x), \quad \tilde{A}_z(x) = \sum_{n=1}^{N} C_{3N+n}\psi_n(x),$$

where $\psi_n(x)$ are the basis functions, and C_j are the corresponding coefficients. The serial indexing of C_j has been chosen for numerical convenience. For simplicity, the basis functions $\psi_n(x)$ are taken to be pyramid functions [29]

$$\psi_n(x) = \begin{cases} \dfrac{x - x_{n-1}}{x_n - x_{n-1}}, & \text{if } x_{n-1} \le x \le x_n \\ \dfrac{x_{n+1} - x}{x_{n+1} - x_n}, & \text{if } x_n \le x \le x_{n+1} \\ 0, & \text{otherwise} \end{cases} \tag{11}$$

for $|x|<L_{\max}$, and $\psi_1(x)=\exp(-\alpha|x-x_1|)$ for $|x|>L_{\max}$, where $L_{\max}$ is chosen such that the solutions are consistent with the Harris sheet boundaries. Here $\alpha=(k_y^2-\omega^2/c^2)^{1/2}$, and $\psi_n(x)$ satisfy the boundary condition that the field perturbations vanish at infinity. Inserting these basis functions into the field equation (10), one obtains

$$M_{ij}C_j = 0, \tag{12}$$

where the elements of the $4N\times 4N$ matrix M_{ij} are computed from the inner product between the N basis functions and the field potentials. The inner product between $\psi_n(x)$ and $g(x)$ is defined by $\langle\psi_n|g\rangle=\int_{-\infty}^{\infty}\psi_n(x)g(x)dx$. Nontrivial solutions to Eq. (12) exist if

$$\det(M_{ij}) = 0, \tag{13}$$

which is the general dispersion relation for linear LHD waves in the inhomogeneous plasma of the Harris sheet. It determines the complex eigenvalues, or the frequency ω, in terms of the wave vector k_y. In the following, we shall solve

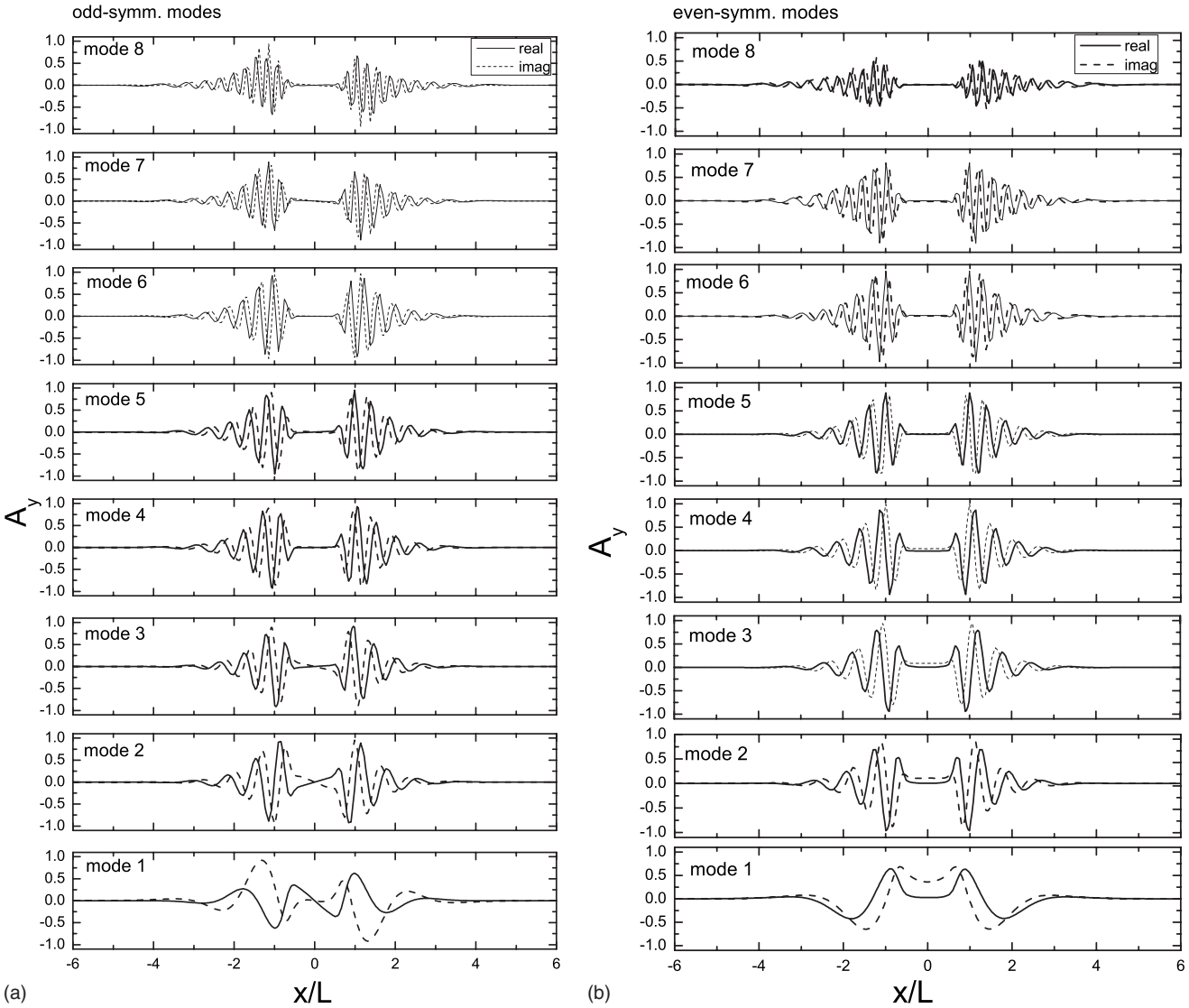

FIG. 1. The vector potential A_y of eight even- and odd-parity eigenmodes for $k_yL=2.0$, $n_{O^+}/n_e=0.1$, and $T_{O^+}=T_e$. The solid and dashed curves denote the real and imaginary parts, respectively, of A_y.

Eq. (13) numerically for the complex frequency ω for fixed k_y, and obtain the corresponding eigenfunctions that determine the mode structure.

IV. NUMERICAL RESULTS

We now investigate the effect of the O^+ ions on the LHDI in the current sheet numerically. For simplicity, we adopt the normalization $x_*=x/L$, $t_*=t/\Omega_{ci}$, $\tilde{\tilde{A}}_*=\tilde{\tilde{A}}/A_0$, and $\tilde{\phi}_*=c\tilde{\phi}/A_0v_{ti}$, where $A_0=-B_0L$ is the characteristic scale of the vector potential and $\Omega_{cs}=q_sB_0/m_sc$ is the gyrofrequency of particles in the asymptotic field B_0. In the numerical calculation, the mass ratio is $m_i/m_e=1836$ and the other parameters are $\rho_i/L=2$, $U_i/v_{ti}=2$, $T_i=T_e=5$ keV, and $L_{max}=5L$, where $\rho_i=v_{ti}/\Omega_{ci}$ is the ion gyroradius.

A. Unstable LHD modes

For fixed k_y, Eq. (13) has different solutions corresponding to LHD modes with different frequencies and different x-direction structures. These modes are analogous to the harmonic modes in a homogeneous plasma, except that here the mode frequencies need not be harmonics of the fundamental frequency. Nevertheless, we can label each mode by a mode number m, and sort m in terms of the magnitude of the real frequency of the corresponding mode. In Fig. 1, the structures of several unstable modes of both even- and odd-parities are shown for $n_{O^+}/n_e=0.1$, $T_{O^+}/T_e=1$, and $k_yL=2.0$ (corresponding to $k_y\sqrt{\rho_i\rho_e}\sim 0.84$). For clarity, we have presented only several typical LHD modes with electromagnetic (in particular, $\tilde{A}_y\neq 0$) components, including the one ($m=4$) having the maximum growth rate. The real and imaginary parts of $\tilde{A}_y$ are denoted by the solid and dashed curves, respectively. The frequency ω as a function of the mode number m is given in Fig. 2, from which one can see that although they do not have the largest amplitude, the odd and even $m=4$ modes have the largest growth rates. Clearly, it should be of interest to investigate the evolution of the

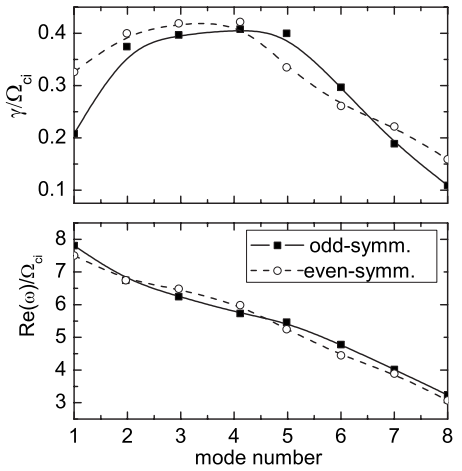

FIG. 2. Real and imaginary parts of the frequencies of the modes shown in Fig. 1. vs the mode number m, for $n_{O^+}/n_e=0.1$, $T_{O^+}=T_e$, and $k_yL=2.0$.

system to see which mode eventually dominates. However, this task is beyond the limitations of the present linear approach.

B. Typical mode structure in the plasma sheet

The scalar and vector potentials for the fastest growing odd-parity $M=4$ mode are shown in Fig. 3. The growth rate and real frequency for this mode are $\mathrm{Im}(\omega)/\Omega_{ci}=0.41$ and $\mathrm{Re}(\omega)/\Omega_{ci}=5.73$, respectively. One can see that the mode is antisymmetric in $\tilde{A}_y$ and $\tilde{\phi}$, but symmetric in $\tilde{A}_x$. The z component $\tilde{A}_z$ $(\sim 10^{-18})$ remains small across the sheet, and the gauge condition is satisfied.

C. Effect of O^+ on the growth rate

We shall now focus mainly on the effects of the O^+ ions on the most unstable eigenmodes. In Fig. 4, the growth rate of the most unstable eigenmodes for $k_yL=2.0$ and $T_{O^+}/T_e=1$ is shown. We note that the growth rate of both the odd- and even-parity modes is not monotonic with respect to the O^+ content: it first decreases with increasing n_{O^+}/n_e, then increases for $n_{O^+}/n_e>0.2$.

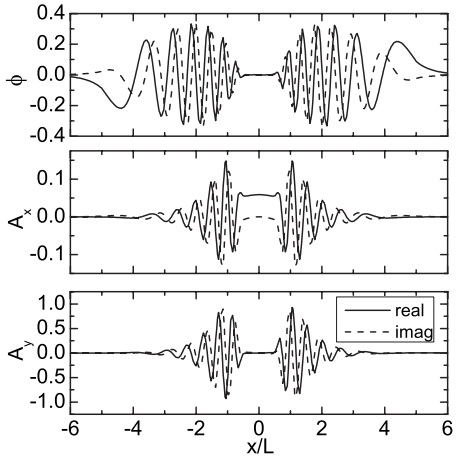

FIG. 3. The eigenfunctions ϕ and $\vec{A}$ of the LHDI mode for $n_{O^+}/n_e=0.1$, $T_{O^+}=T_e$, and $k_yL=2.0$.

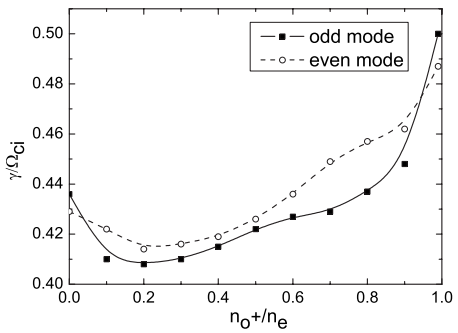

FIG. 4. The growth rate of the fastest growing LHD modes as a function of n_{O^+}/n_e for $T_{O^+}=T_e$ and $k_yL=2.0$. Solid lines denote the odd-parity modes and dashed lines the even-parity modes.

When the O^+ ions dominate the plasma sheet, the growth rate of the LHDI in the current sheet can be considerably higher than that in a plasma without O^+ ions. The latter can dominate a plasma sheet during magnetic substorms and reconnections [31,32]. When the O^+ concentration is low, the energy transfer is mainly between the H^+ ions and the LHD waves. As the O^+ content increases, energy transfer between the O^+ ions and the LHD waves also increases and eventually exceeds that of the H^+ ions. At a certain O^+ content, the total energy transfer by Landau damping between the LHD waves and the O^+ and H^+ ions attains a maximum, resulting in a minimum in the growth rate, as can be seen in Fig. 4. Figure 5 shows the influence of T_{O^+}/T_e on the growth rate of the fastest growing LHD modes for $k_yL=2.0$ and $n_{O^+}/n_e=0.65$. The variation in the growth rate with T_{O^+}/T_e for both the odd- and even-parity modes has nearly the same tendency: it first decreases rapidly until $T_{O^+}/T_e=2.3$, then it increases slowly. The existence of a minimum can be physically expected since when the O^+ ions dominate the plasma sheet, they are mainly responsible for the wave-particle energy transfer. Accordingly, as the O^+ temperature increases, Landau damping due to the O^+ ions also increases until a peak is reached, corresponding to the minimum in the growth rate, as seen in Fig. 5.

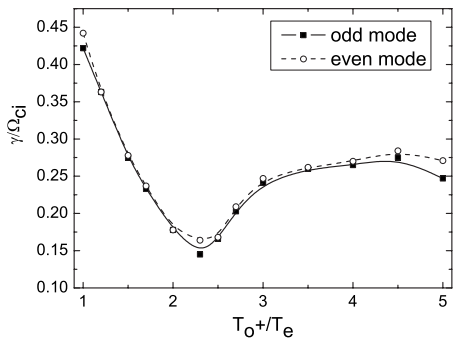

FIG. 5. The growth rate of the fastest growing LHD modes as a function of T_{O^+}/T_e for $n_{O^+}/n_e=0.65$ and $k_yL=2.0$. Solid lines denote the odd-parity modes and dashed lines the even-parity modes.

V. DISCUSSION

Using Vlasov theory, we have studied the effect of O^+ ions on the LHDI with intermediate-wavelength $k_y\sqrt{\rho_i\rho_e}\sim 1$, such that the LHD mode has a significant electromagnetic component that might affect the onset of magnetic reconnection [18]. Our results show that there exists multiple harmonics of unstable eigenmodes with both even and odd parity. The growth rate of the fastest growing mode is not monotonic with the O^+ (heaviest species) content and temperature. In a sense, this result is in contrast with earlier studies of the effect of particle mass and temperature ratios in two-species plasmas, which showed that the growth rates of the magnetic instabilities decrease monotonically with the ion-to-electron mass and temperature ratios [28,33]. In a plasma with O^+ ions, the competitive interactions between the waves and the O^+ and H^+ ions can lead to a nonmonotonic variation in the growth rate with the O^+ content and temperature. This is because the total energy transfer between the O^+ and H^+ ions and the waves depends on the concentration of these ions. In fact, it is found that there can exist a minimum in the net growth rate for certain O^+ content. On the other hand, as T_{O^+} increases, the O^+-ion Landau damping will attain a maximum before it decreases with further increase in T_{O^+}. Thus, the growth rate can also have minimum with respect to T_{O^+}. Since the LHDI in the three-species plasma can have much larger growth rates than that in a two-component plasma, it can be responsible for the occurrence of magnetic reconnection in the Harris sheet, especially when the O^+ content is significant.

ACKNOWLEDGMENT

This work was supported by the National Natural Science Foundation of China (Projects No. 10775134, No. 10831062, and No. 10835003).

[1] A. G. Elfimov, J. A. Tataronis, and N. Hershkowitz, Phys. Plasmas **1**, 2637 (1994).
[2] K. Appert *et al.*, Plasma Phys. Controlled Fusion **28**, 133 (1986).
[3] W.-Q. Li, D. W. Ross, and S. M. Mahajan, Phys. Fluids B **1**, 2364 (1989).
[4] M. Hesse and J. Birn, Ann. Geophys. **22**, 603 (2004).
[5] R. M. Winglee, J. Geophys. Res. **109**, A09206 (2004).
[6] W. K. Peterson *et al.*, J. Geophys. Res. **87**, 2139 (1982).
[7] K. Seki *et al.*, J. Geophys. Res. **103**, 4477 (1998).
[8] K. N. Ostrikov, S. V. Vladimirov, and M. Y. Yu, J. Geophys. Res. **104**, 593 (1999).
[9] Y. H. Chen, W. Lu, and M. Y. Yu, Phys. Rev. E **61**, 809 (2000).
[10] K. Seki *et al.*, Science **291**, 1939 (2001).
[11] K. Seki *et al.*, J. Geophys. Res. **107**, 1047 (2002).
[12] A. B. Galvin *et al.*, Space Sci. Rev. **136**, 437 (2008).
[13] E. Echer *et al.*, J. Geophys. Res. **113**, A05209 (2008).
[14] J. Birn, M. F. Thomsen, and M. Hesse, Ann. Geophys. **22**, 1305 (2004).
[15] O. J. G. Silveira *et al.*, Phys. Rev. E **65**, 036407 (2002).
[16] E. G. Harris, Nuovo Cimento **23**, 115 (1962); W.-Z. Fu and L.-N. Hau, Phys. Plasmas **12**, 070701 (2005).
[17] P. H. Yoon, Y. Lin, X. Y. Wang, and A. T. Y. Lui, Phys. Plasmas **15**, 112103 (2008).
[18] W. Daughton, Phys. Plasmas **10**, 3103 (2003).
[19] I. Silin, J. Bunchner, and A. Vaivads, Phys. Plasmas **12**, 062902 (2005).
[20] N. Krall and P. Liewer, Phys. Rev. A **4**, 2094 (1971).
[21] J. D. Huba, J. F. Drake, and N. T. Gladd, Phys. Fluids **23**, 552 (1980).
[22] J. D. Huba and C. S. Wu, Phys. Fluids **19**, 988 (1976).
[23] R. C. Davidson and N. T. Gladd, Phys. Fluids **18**, 1327 (1975).
[24] G. S. Lakhina and A. Sen, Nucl. Fusion **13**, 913 (1973).
[25] Y. M. Zhou *et al.*, J. Geophys. Res. **88**, 3026 (1983).
[26] P. Ricci *et al.*, Phys. Plasmas **12**, 055901 (2005).
[27] Y. Wang, R. Kulsrud, and H. Ji, Phys. Plasmas **15**, 122105 (2008).
[28] W. Daughton, Phys. Plasmas **6**, 1329 (1999).
[29] J. P. Boyd, *Chebyshev and Fourier Spectral Methods* (Dover, New York, 2000), p. 346.
[30] P. H. Yoon, A. T. Y. Lui, and R. B. Sheldon, Phys. Plasmas **13**, 102108 (2006).
[31] L. M. Kistler *et al.*, J. Geophys. Res. **110**, A06213 (2005).
[32] Y. Yao *et al.*, J. Geophys. Res. **113**, A04220 (2008).
[33] G. Lapenta and J. U. Brackbill, Phys. Plasmas **9**, 1544 (2002).